Air Distribution in Rooms, (ROOMVENT 2000)
Editor: H.B. Awbi

THE USE OF SOLAR AIR COLLECTORS FOR ROOM VENTILATION: A STUDY USING TWO NUMERICAL APPROACHES

A. Moret Rodrigues[1]; A. Canha da Piedade[1]; H. B. Awbi[2]

[1]*Instituto Superior Técnico/ICIST - Av. Rovisco Pais, 1049-001 Lisbon, PORTUGAL*

[2]*Department of Construction Management & Engineering, The University of Reading, UK*

ABSTRACT

Solar energy air-collectors installed on the sun-oriented building façades can be used for improving natural ventilation of adjacent rooms. The basis of the physical process is an unbalanced buoyancy force arising from the temperature difference between ambient and the air inside the room. Although difficult to control due to the variability of the climatic conditions, these devices can be used as means of reducing the need for conventional energy to provide indoor air conditions within acceptable limits required by health and comfort considerations. In this paper, two numerical approaches of different complexity are applied to study the airflow produced by a solar-air collector in a room. These are a simplified model, based on the integral equations of motion and Bernoulli theorem, which provides an insight into the main features of the flow, and a more complex computational fluid dynamics (CFD) model called VORTEX. The simplified model takes into consideration the heat and momentum transfer within the collector and room and the CFD code used has been specifically developed for studying the air movement in rooms, which solves the full elliptic Navier-Stokes equations together with the equations for the k-ε turbulence model. Results for a parametric study of a room with an air collector using both models are presented and discussed.

KEYWORDS: Solar air-collector, Integral flow equations, CFD model, Natural ventilation, Room air movement

INTRODUCTION

This paper analyses the behaviour of solar-air collectors used as passive devices contributing to comfort and health requirements in rooms. Specifically, the solar-air collector design used in this study is mainly for providing room air ventilation for the following two purposes:

- *Winter time:* to reduce the pollutant concentration of room air by preheating incoming air thereby reducing the heat losses associated with the ingress of outdoor cold air.

- *Summer time:* to increase the ventilation rates to the room through open windows by buoyancy action during the day.

This is an important application area in buildings of high occupancy density that normally require a mechanical ventilation system but where costs associated with such mechanical devices (capital and maintenance) are important barriers to their practical implementation. That is the case of school buildings (classrooms) in some countries (Moret Rodrigues *et al.*, 1996).

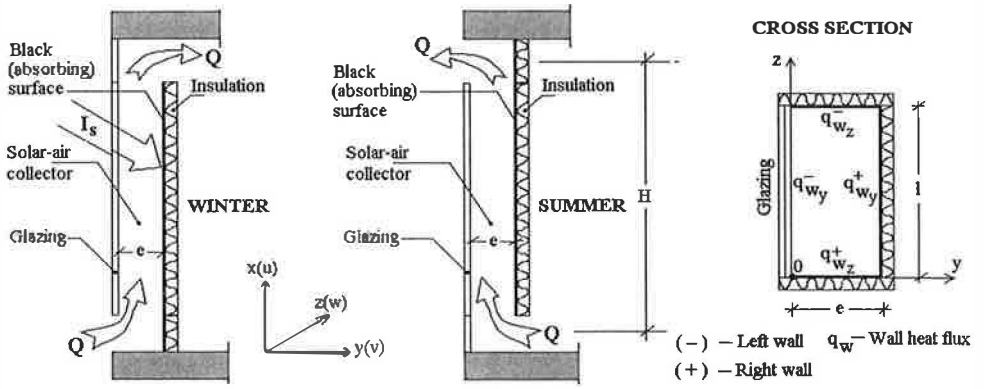

Fig. 1: Solar-air collector

The solar-air collector is basically composed of four walls forming a gap, with different functions: The external wall is a glazing, transparent to the short wave radiation (solar irradiation, I_s , Fig. 1); the internal walls are energy absorbing, by the use of a black covering sheet (absorber) on the exposed surface and made of a light insulation material. A low thermal inertia and a high level of insulation result in higher temperatures, larger heat gain to the air within the gap, and a consequent increase in the collector performance.

In winter, the outdoor air entering the collector through a lower opening is heated by contact with the absorber and the density differences produce the driving force ("stack effect") that pulls the air upwards into the room through an opening at the top of the channel (Fig. 1, winter case). Complementarily to the collector, a chimney is used in the opposite side as a path for extracting the room air, with or without the help of a fire placed at its base.

In summer, during the day, the system induces air circulation in the reverse direction to the winter case, as shown in Fig. 1 (summer case), through inlets placed on the opposite façade. At night, the system works as an extract with the fresh air entering the room through openings thus removing the heat accumulated in the enclosed space.

A simple method based on integral equations and Bernoulli theorem is developed and applied to the problem of the channel coupled with the room and chimney, in winter, and with the room and windows, in summer. This will be useful in understanding the basic parameters that govern the flow and in helping designers in their study of similar problems, mainly in the first stages of the design process. In parallel, CFD simulations are presented and results compared. This will be useful in supporting the simple model and in providing an insight of the flow within the room.

INTEGRAL MODEL

The basic model applies the steady-state, isotropic 3-D turbulent boundary layer equations of momentum, mass continuity and energy, respectively given by

$$\frac{\partial(\rho u u)}{\partial x}+\frac{\partial(\rho v u)}{\partial y}+\frac{\partial(\rho w u)}{\partial z}=\frac{\partial}{\partial y}\left(\mu_e\frac{\partial u}{\partial y}\right)+\frac{\partial}{\partial z}\left(\mu_e\frac{\partial u}{\partial z}\right)-\frac{\partial p}{\partial x}-\rho g \tag{1}$$

$$\frac{\partial(\rho u)}{\partial x}+\frac{\partial(\rho v)}{\partial y}+\frac{\partial(\rho w)}{\partial z}=0 \tag{2}$$

$$\frac{\partial(\rho u T)}{\partial x}+\frac{\partial(\rho v T)}{\partial y}+\frac{\partial(\rho w T)}{\partial z}=\frac{\partial}{\partial y}\left(\Gamma_e\frac{\partial T}{\partial y}\right)+\frac{\partial}{\partial z}\left(\Gamma_e\frac{\partial T}{\partial z}\right) \tag{3}$$

to a nearly constant density flow in a rectangular duct (x - diffusion terms dropped for being of minor importance) – with height H and perimeter $\chi=2(1+e)$ – subjected to a uniform heat flux (Neumann conditions) $q_w=\left[1\left(q_{w_y}^-+q_{w_y}^+\right)+e\left(q_{w_z}^-+q_{w_z}^+\right)\right]/\chi$ – on the solid boundaries. In these equations the effective viscosity is $\mu_e=\mu+\mu_t$ and the effective diffusion coefficient is $\Gamma_e=\mu_e/\sigma_e$; μ_t being the turbulent viscosity and σ_e the effective Prandtl number. Equations 1~3 are firstly integrated over the channel area $S=1\times e$. At the wall boundaries, the no-slip conditions $u=v=w=0$ apply and, for the derivatives, the apparent shear stresses $\tau_{app_i}=\mu_e\partial u/\partial x_i$ and apparent heat fluxes $q_{app_i}=-c_p\Gamma_e\partial T/\partial x_i$ are equal to the wall values, τ_{w_i} and q_{w_i} respectively $(i=1,2,3)$. From the integration of Eqn. 2 it is found that the mass flux $\dot{m}=\int_S\rho u\,dS$ is constant over the channel height. Using averaged quantities, $u_s=\int_S u\,dS/S=Q_s/S$, $p_s=\int_S p\,dS/S$, $\rho_s=\int_S\rho\,dS/S$, Q_s being the air flow rate, and following the notation of Fig. 2, a second integration of Eqn. 1 over the channel height gives, for the winter case:

$$p_{s,2}=p_{s,1}-\frac{2\rho_e Q^2}{D_{co}S_{co}^2}\int_1^2 c_{fco,x}dx-g\int_1^2\rho_{s,x}dx \tag{4}$$

where the fully developed flow and Boussinesq approximations (a constant axial velocity and density variations only affecting the buoyancy term, respectively) are used and the concepts of hydraulic diameter $D\equiv 4\times S/\chi=2\times(1\times e)/(1+e)$ and shear stress coefficient $c_f=2\tau_w/(\rho_s u_s^2)$, are also introduced. Using, for the density variation, the relationship $\rho_{s,x}=\rho_e\left[1-\beta(T_{s,x}-T_e)\right]$, where $\beta=1/T_e$ is the coefficient of thermal expansion and $T_s=\int_S\rho u T dS/\dot{m}$ is the channel bulk temperature, a second integration of Eqn. 3 gives $T_{s,x}=T_{s,1}+\psi x$, with $\psi=2q_w(1+e)/(\rho_e Q c_p)$. Thus, the buoyancy integral term of Eqn. 4 results in

$$\int_1^2\rho_{s,x}dx=\rho_e H_{co}\left(1-\beta\psi\frac{H_{co}}{2}\right) \tag{5}$$

For turbulent flow, $c_f=0.079\,Re_D^{-1/4}$ $\left(2\times10^3<Re_D<2\times10^4\right)$ (Bejan,1993) is adopted, with the Reynolds number given by $Re_D=QD/(S\nu)$, and the correspondent integral of Eqn. 4 can easily be solved. At the inlet, the flow contraction gives rise to a minor loss that can be expressed as:

$$p_{ref,e}-p_{s,1}=\frac{\rho_e}{2}\left(\frac{Q}{C_{dco}A_{co}}\right)^2 \tag{6}$$

which is obtained by applying the Bernoulli theorem. Here, $p_{ref,e}$ is the external reference pressure, A is the inlet area of the collector and C_d is the discharge coefficient. In turn, at the outlet, and since the streamlines are approximately parallel, the static pressure across the jet can be assumed as:

$$p_{s,2} = p_3 \tag{7}$$

and assuming still room air,

$$p_3 = p_{ref,i} - \rho_i g H_{co} \tag{8}$$

where $p_{ref,i}$ is the internal reference pressure. The chimney will be simply assumed as an air extract system. This means that the chimney only contributes to the flow in terms of energy loss. At a more advanced stage of the study a fire at the base of the chimney can also be included in winter to add an additional heat source and assist the ventilation induced by the collector. Applying Eqn. 4 to this case gives (Fig. 2):

$$p_{s,5} = p_{s,4} - \frac{2\rho_i Q^2 c_{fch} H_{ch}}{D_{ch} S_{ch}^2} - \rho_i g H_{ch} \tag{9}$$

similarly,

$$p_{s,5} = p_6 ; \quad p_6 = p_{ref,e} - \rho_e g H_{ch} ; \quad p_{ref,i} - p_{s,4} = \frac{\rho_i}{2}\left(\frac{Q}{C_{dch} A_{ch}}\right)^2 \tag{10}$$

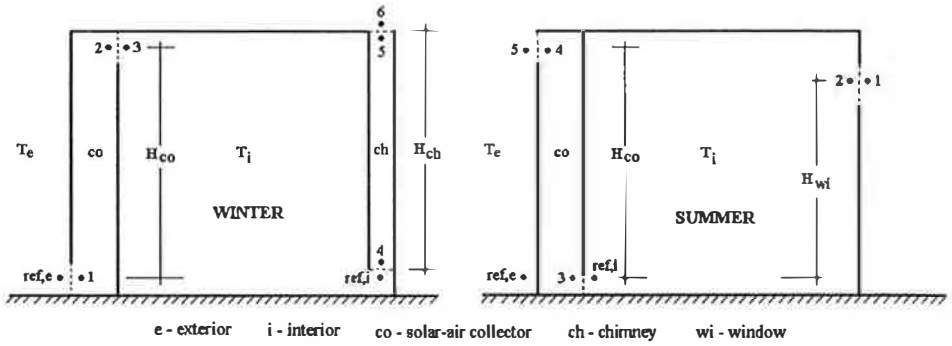

Fig. 2: Integral model

Combining Eqns. 4–10, with $\rho_i = \rho_e$, the flow rate in the winter case is given by the implicit equation

$$Q = \sqrt{\frac{g\beta\psi H_{co}^2}{\left(\frac{1}{C_{dco} A_{co}}\right)^2 + \left(\frac{1}{C_{dch} A_{ch}}\right)^2 + \frac{4 c_{fco} H_{co}}{S_{co}^2 D_{co}} + \frac{4 c_{fch} H_{ch}}{S_{ch}^2 D_{ch}}}} \tag{11}$$

The construction of the model for the summer case is identical to the winter case, with one difference and that is the chimney does not take part in the ventilation process but is replaced by one or more open windows (j=1,..n) at a height H_{wi}. In this case, it is easy to conclude that the relevant equation becomes:

$$Q = \sqrt{\frac{g\beta\psi H_{co}^2}{\left(\frac{1}{C_{co} A_{co}}\right)^2 + \left(\frac{1}{\sum_j C_{dwi_j} A_{wi_j}}\right)^2 + \frac{4 c_{fco} H_{co}}{S_{co}^2 D_{co}}}} \tag{12}$$

CFD MODEL

The CFD study was carried out using a 3-D computer code - VORTEX (Awbi,1996) - which numerically solve the differential equations that govern air movement – continuity, momentum and thermal energy equations - for the combined flow in the room and other systems considered here. The program allows for the turbulent nature of the flows by solving two additional equations for the kinetic energy and energy dissipation rate which are the base of the so-called $\kappa-\varepsilon$ turbulence model. The numerical scheme uses a staggered 3-D Cartesian system where equations are discretized using the Finite Volume Method (FVM) and solved by the well known SIMPLE algorithm. To enhance the stability of the solution process under-relaxation techniques are applied to all the equations. This program has been extensively validated in solving various types of ventilation flows.

RESULTS AND DISCUSSION

The following figures present results for the cases tested, either from the integral model (INT), based on equations (11) and (12), or from the CFD model, based on the numerical solution of the flow equations. The simulations were carried out for a room size of 5m x 5m x3.2m, collector and chimney heights of H_{co}=2.9m and H_{ch}=2.7m, respectively, collector and chimney sections of S_{co}=0.2m x 0.7m and S_{ch}=0.3m x 0.3m, and opening areas of A_{co}=0.3m x 0.7m for the collector and A_{ch}=0.3m x 0.3 m for the chimney.

In Fig. 3, the variation of the air flow rate with the heat flux on the absorbing collector walls (set equal for both, i.e., $q^+_{w_y} = q^-_{w_z} = q^+_{w_z}$) is shown for both models in the two working situations considered, i.e. summer (S) and winter (W). For the summer situation, the results shown correspond to the case of two open windows of area A_{wi}=0.70m x 0.70m each, positioned at a height H_{wi}= 2.0m on the wall opposite the collector. The corresponding curves have similar trends, with a progressive increase of airflow rate with the flux intensity, and the agreement achieved is very satisfactory considering the difference in complexity between the two models. It is important to note that despite the fact that the heating power has been set the same for the winter and summer cases, the corresponding air flow rates are different. The lower values in winter are due to the higher resistance offered to the flow by the chimney device when compared to the minor losses produced by the windows in summer.

In Figs. 4~7 some of the CFD plots are shown for both winter and summer situations. Figs. 4 and 5 are referred to the same winter simulation case: T_e=15 °C and $q^+_{w_y} = q^-_{w_z} = q^+_{w_z}$=100 W/m^2. In Fig. 4 the contour lines of the air temperature for a longitudinal plane in the middle of the room are plotted. The higher values observed at the collector outlet are followed by a progressively decreasing temperature with distance from the collector, on one hand, and the distance from the ceiling, on the other. This stratification is consistent with the corresponding flow patterns shown in Fig. 5.

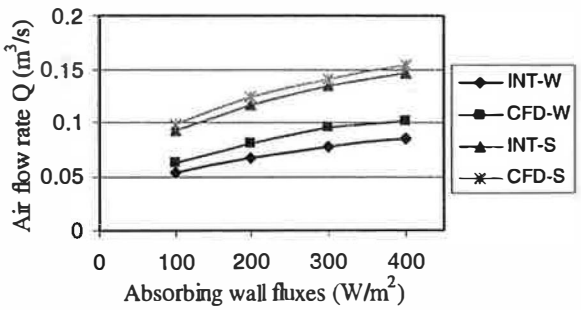

Fig. 3: Air flow rates

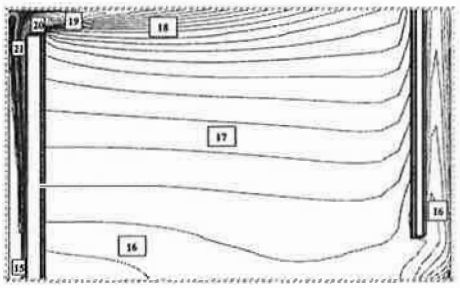

Fig. 4: Temperature distribution in a middle section (W)

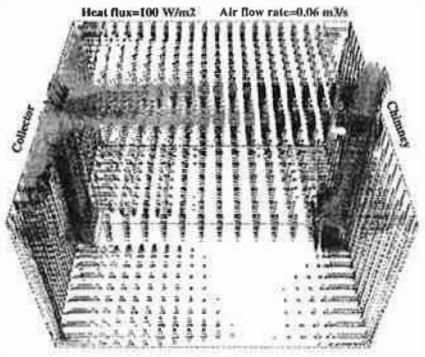

Fig. 5: Velocity distribution (W)

In the winter case, a typical situation is a warm jet leaving the channel at the top and moving towards the direction of the chimney close to the ceiling (Fig. 5). Conversely, when the flow enters through the windows (summer case), the lower velocities at inlet causes the jet to drop soon after entrance, thus resulting in a more efficient air distribution in the occupied zone (Figs. 6 and 7).

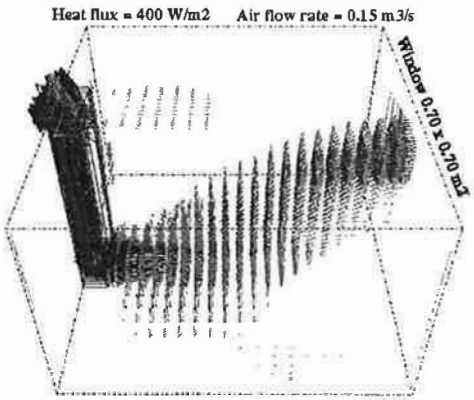

Fig. 6: Air velocities - single window (S)

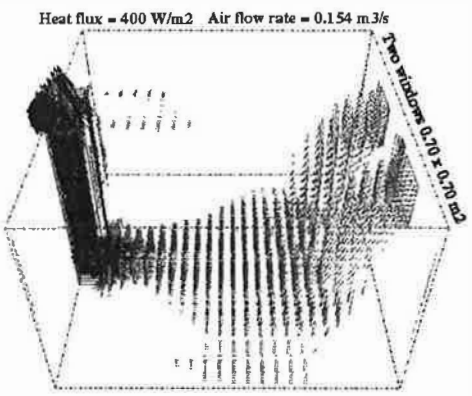

Fig. 7: Air velocities - two windows (S)

To predict the distribution of CO_2 in the room the same numerical procedure described above for velocity and temperature was used but where an additional transport equation for the concentration was solved. Sixteen CO_2 sources representing seated people were uniformly distributed through the room at height of 1.35m above the floor, with each producing 4.7×10^{-3} l/s (total production $P = 75.2\times10^{-3}$ l/s), and an average outdoor air concentration of $\overline{C}_e = 0.4\times10^{-3}$ (400 ppm) was considered. A graphical representation of the concentration at this height is shown as horizontal planes in Figs. 8 and 9 and also for the sections C1 and C2 in Fig. 10. The mean concentration in the occupied zone $\overline{C}_{oc}$ (from floor to 1.8 height) and in the whole space $\overline{C}_{sp}$ are lower than the recommended limits for comfort and health (Portuguese recommendation for a period of one hour: 1.2×10^{-3}) although locally they are exceeded (Fig.10). Despite the fact that the two flow rates are nearly the same, the two windows give higher ventilation effectiveness as shown from the results of Figs. 8 ~ 10. The mean velocities for the occupied zone $\overline{V}_{oc}$ and for the whole space $\overline{V}_{sp}$ are also below the comfort limit (ASHRAE Standard 55-1992 recommends 0.25 m/s for summer).

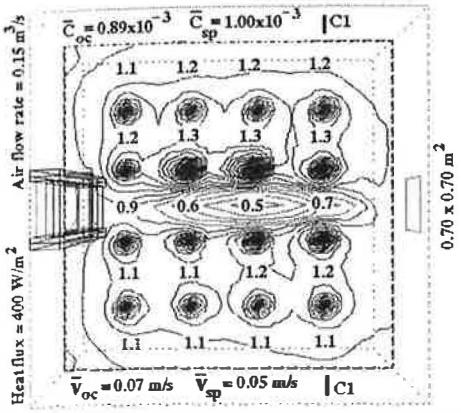

Fig. 8: CO_2 contours (x10^{-3}) (single window)

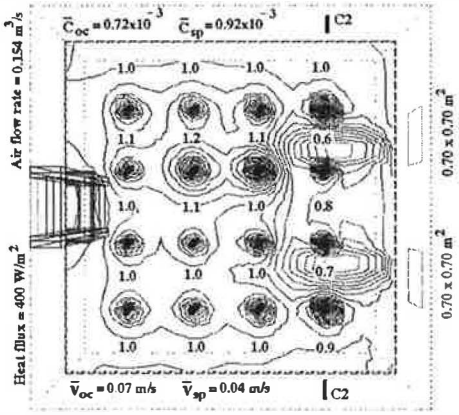

Fig. 9: CO_2 contours (x10^{-3}) (two windows)

Prolonging the use of the simplified method to the evaluation of the mean concentration, it is useful to compare the CFD value with that obtained through the simple equation, valid for the stationary state,

$$(\bar{C}_{sp} - \bar{C}_e) \times Q = P$$

With $P = 75.2 \times 10^{-3}$ l/s, C_e=0.4x10^{-3}, Q=0.147x10^3 l/s (INT model value – Fig. 3 - for a heat flux on the absorbing walls of 400 W/m^2) one easily conclude that the concentration value that there results, that is $\bar{C}_{sp} = 0.91 \times 10^{-3}$, agrees very well with that predicted by the CFD model (Figs. 8 and 9).

CONCLUSIONS

A simple model for room ventilation based on integral equations was developed and compared with a more complex CFD model. The agreement of results from the two models is very encouraging for so that the simple model could be used as first step in the design of these solar ventilators. The CFD simulation was undertaken in order to obtain detailed information about the flow. These results also seem feasible for the conditions being simulated in this study.

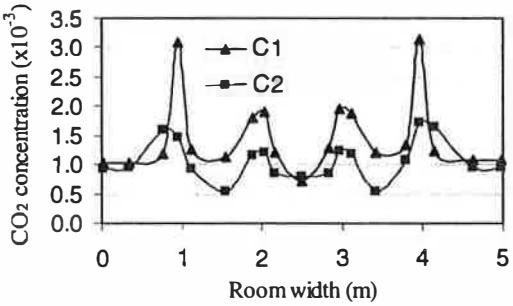

Fig. 10: CO_2 distribution (C1 and C2 in Figs. 8 and 9 respectively)

REFERENCES

ASHRAE Standard 55-1992 (1992). *Thermal Environment Conditions for Human Occupancy*, ASHRAE, Atlanta, USA.

Awbi, H.B. (1996). VORTEX-2, A Computer code for Air Flow, Heat Transfer and Concentration in Enclosures, version 2.1, U.K.

Bejan, Adrian (1985). *Heat Transfer*, John Wiley & Sons, Inc., New York.

Moret Rodrigues, A., A. Canha da Piedade, S. Domingos and S. Valente Pereira (1996). Performance of solar-air collectors for classroom ventilation: Mathematical models versus experimental results. In: Proceedings of the 4th European Conference *Solar Energy in Architecture and Urban Planning*, pp. 472-475, Berlin.